JOURNAL OF AGRICULTURAL AND FOOD CHEMISTRY

Article

pubs.acs.org/JAFC

Temperature-Dependent Raman Spectroscopic Evidence of and Molecular Mechanism for Irreversible Isomerization of β-Endosulfan to α-Endosulfan

Walter F. Schmidt, Cathleen J. Hapeman,* Laura L. McConnell, Swati Mookherji, Clifford P. Rice, Julie K. Nguyen, Jianwei Qin, Hoyoung Lee, Kuanglin Chao, and Moon S. Kim

Agricultural Research Service, United States Department of Agriculture, 10300 Baltimore Avenue, Beltsville, Maryland 20705-2325, United States

ABSTRACT: Endosulfan (6,7,8, 9,10,10-hexachloro-1,5,5a,6,9,9a-hexahydro-6,9-methano-2,4,3-benzodioxathiepine-3-oxide) is a broad-spectrum, organochlorine insecticide used on numerous crops since the 1950s. It is has been identified as a persistent organic pollutant (POP) due to its persistence, bioaccumulation, long-range transport, and adverse effects to human health and aquatic ecosystems; it will be phased out in the United States in 2016. Endosulfan consists of two diastereomers, α and β; α-endosulfan exists as two asymmetrical, twist-chair enantiomers which interchange, while β-endosulfan has a symmetrical-chair conformation. β-Endosulfan has been shown to isomerize to α-endosulfan. Here we document the previously proposed isomerization mechanism using temperature-dependent Raman (TDR) spectroscopy. The bending frequencies in the fingerprint region were assigned to specific bonds. Changes in the signal intensity as a function of temperature were used to identify detailed ring movements and thus conversion of β to α. These movements cannot occur simultaneously nor symmetrically, precluding conversion of α-endosulfan to β-endosulfan.

KEYWORDS: *endosulfan (6,7,8,9,10,10-hexachloro-1,5,5a,6,9,9a-hexahydro-6,9-methano-2,4,3-benzodioxathiepine-3-oxide), 1,3-dioxepane, temperature-dependent Raman (TDR) spectroscopy, 2D-TDR spectra, Raman ring-bending frequency, temperature-dependent conformational changes*

INTRODUCTION

Endosulfan (6,7,8, 9,10,10-hexachloro-1,5,5a,6,9,9a-hexahydro-6,9-methano-2,4,3-benzodioxathiepine-3-oxide) is a broad-spectrum organochlorine insecticide that has been used on cereals, fruits, vegetables, and cotton since the 1950s.[1,2] It exists as two diasteromers, α-endosulfan and β-endosulfan, and is typically applied to crops as a 70:30 isomeric ratio of α:β. In 2010, the United States Environmental Protection Agency initiated a Memorandum of Agreement to phase out all uses of endosulfan completely by July 2016 because of the unacceptable risks to farm workers and wildlife and because it can persist in the environment.[3,4] The United Nations Environmental Programme (UNEP), Parties to the Stockholm Convention on Persistent Organic Pollutants (POPs), agreed to list endosulfan as a POP in 2011.[5] Numerous reviews have documented studies concerning the persistence, bioaccumulation, long-range transport, and adverse effects to aquatic ecosystems and to human health posed by endosulfan [e.g., refs 6−8]. Despite the virtual global ban on endosulfan, the environmental fate of these two compounds will remain a global issue long after their use has ceased.

The chemical structure of both endosulfan isomers has been examined and disputed extensively since it was first patented in 1958.[9−12] More recent research confirmed that β-endosulfan is symmetrical as previously suggested but that α-endosulfan is actually composed of two asymmetrical enantiomers (Figure 1).[13] Additional research concerning the Henry's Law Constants of endosulfan led to the discovery that β-endosulfan readily converts to α-endosulfan in the aqueous phase.

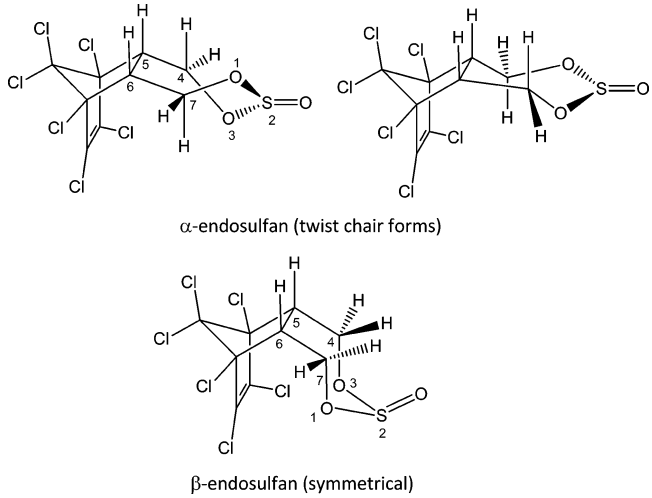

Figure 1. Structure of both enantiomers of α-endosulfan and β-endosulfan. For brevity, atom numbers are assigned only to the seven-membered dioxathiepine-3-oxide system, beginning from oxygen site. The β-endosulfan molecule is symmetrical; α-endosulfan is asymmetrical.

Received: September 30, 2013
Revised: January 31, 2014
Accepted: February 3, 2014
Published: February 3, 2014

Experiments were conducted using a wetted-wall column to examine the partitioning of the nearly pure endosulfan isomers from water into air. When starting with β-endosulfan, α-endosulfan was virtually the only isomer observed in air phase.[14,15] In regional and long-range transport studies of endosulfan isomers in air, β-endosulfan was infrequently observed relative to α-endosulfan, so much so that it was disregarded in the data analyses.[16,17] The isomerization of β-endosulfan to α-endosulfan has been suggested as a possible reason for the observed overabundance of α-endosulfan in the atmosphere.[6,18] Finally, this isomerization has also been observed directly on surfaces.[19]

A mechanism for β-endosulfan conversion to α-endosulfan and its irreversibility have been proposed and has been supported with data from differential scanning calorimetry (DSC) and NMR experiments and from computational chemistry calculations.[18] DCS scans of pure α-endosulfan, pure β-endosulfan, and mixtures were acquired; temperatures ranged from 25 to 280 °C. Scans of mixtures showed a large phase transition not observed in either of the pure isomer scans, suggesting a new transition which we assigned to the isomerization process. Furthermore, analysis of the remaining material after the scans revealed a eutectic mixture of an approximately 60:40 mixture of the α:β isomers, again demonstrating conversion. No degradation other than isomeric conversion was observed. Using computational chemistry, a mechanism was proposed whereby movement of the S═O moiety followed pseudorotation of the seven-membered ring of β-endosulfan resulted in formation of α-endosulfan. Furthermore, we concluded that the increase in entropy caused by the asymmetry in α-endosulfan precluded the reverse process of α-endosulfan conversion to β-endosulfan.

The three mixtures of endosulfan (nearly pure α-endosulfan, nearly pure β-endosulfan, and mixtures) have identical chemical compositions, i.e., they differ only in spatial arrangement of the atoms, yet the phase transitions observed using DSC were markedly different in all three mixtures.[18,20] This indicates that the thermal energy is absorbed by different sets of atoms. In addition, DSC does not identify which part of the molecule or bond(s) absorb the thermal energy. Raman spectroscopy provides spectral evidence (frequency signals) identifying the sets of atoms or bonds which are affected by energy absorption. Using the technique of temperature-dependent Raman (TDR) spectroscopy recently developed in our laboratory, molecular sites which respond most strongly to the thermal temperature gradient can be identified. Frequencies which covary with intensity and/or wavenumber shift starting at a specific temperature can indicate the individual molecular site or molecular movement that triggers a reversible or irreversible transition event. From these data, the sequence of molecular movements absorbing a threshold amount of thermal energy can be organized to explain the mechanism of a transition event. The purpose of this article is to provide such evidence that, in concert with previous work, demonstrates the molecular level pathway through which phase transition events occur, particularly, the irreversible process of β-endosulfan converting to α-endosulfan.

MATERIALS AND METHODS

Materials. Certified analytical grade Thiodan (α:β-endosulfan 60:40), β-endosulfan (nearly 100%), and α-endosulfan (99.8% α; 0.2% β) were each obtained commercially from ChemServices (West Chester, PA) and used as is.

Temperature Dependent Raman Measurement System. A Raman spectroscopy system was assembled to collect temperature dependent Raman (TDR) spectra from the samples. A 16-bit CCD camera with 1024 × 256 pixels (Newton DU920N-BR-DD, Andor Technology, South Windsor, CT) was used to acquire Raman scattering signals. A Raman spectrometer (Raman Explorer 785, Headwall Photonics, Fitchburg, MA) was mounted to the camera. The spectrometer accepts light through an input slit (5 mm long × 100 μm wide) and detects a Raman shift range of 102.2−2538.1 cm^{-1} with a spectral resolution of 3.7 cm^{-1}. A 785 nm laser module (I0785MM0350MF-NL, Innovative Photonic Solutions, Monmouth Junction, NJ) served as the excitation source. A fiber optic Raman probe (RPB, InPhotonics, Norwood, MA) was used to focus the laser and acquire the Raman signals. A bifurcated fiber bundle was used to deliver the laser light to the probe and transfer the collected Raman signals to the spectrometer.

A hot plate with a ceramic top surface (Isotemp, Fisher Scientific, Hampton, NH) was used to heat the samples. The powder samples were put in a copper sample holder. Two thermocouple probes (type K) were attached to two sides of the sample area, and they were connected to a dual-input thermometer (EasyView EA15, Extech Instruments, Nashua, NH) to measure the temperature of the samples. Average values of the two probes were used as the sample temperature, and the data were transferred to a computer via a RS-232 port. A copper heat sink was placed between the ceramic heat surface and the sample holder to slow down the speed of the temperature increase. A relatively high temperature resolution was consequently achieved for the temperature-dependent Raman data. The Raman probe, the hot plate, and the sample materials were placed in a closed black box to avoid the influence of ambient light. System software was developed using LabVIEW (National Instruments, Austin, TX) to fulfill functions such as camera control, data acquisition, temperature measurement, and synchronization.[21] Each experiment was conducted in triplicate. Over 200 spectra of 1600 data points were collected for each experiment, resulting in a data set of approximately 10^6 data points.

RESULTS AND DISCUSSION

Raman Spectra Mode Assignments for Each Isomer. Endosulfan consists of two structural parts, a hexachlorinated norboryl moiety and a seven-membered, dioxathiepine-3-oxide ring system. The norbene portion is rigid, which is reflected in the absence of C−Cl Raman vibrational modes except for one signal at 374 cm^{-1}.[22] Vibrational frequencies characteristic of seven-membered ring structures, including cycloheptane and 1,3-dioxepane, have been identified.[21] The seven atoms of these simpler ring systems gave rise to eight ring-bending frequencies, four symmetrical and four asymmetrical. The seven-membered ring in the endosulfan isomers is a structural analogue of 1,3-dioxepane and, correspondingly, the same eight frequencies apply. For brevity, the same numbering of ring atoms in 1,3-dioxepane are used here: the ring oxygen atoms are atoms 1 and 3, sulfur is atom 2, the methylene carbons are C4 and C7, and the methine carbons are C5 and C6 (Figure 1).

The difference in the relative orientation of the axial hydrogens on the methylene carbons, C4 and C7, is responsible for the three discrete forms of endosulfan. In β-endosulfan, one hydrogen atom on each of the methylene carbons is axial above the seven-membered ring system, affording a symmetrical molecule in which $CHCH_2O$ on the right half of the ring is in the same conformation as the left half. This contrasts with the two α-endosulfans, where only one hydrogen atom is axial above the ring, not both, i.e., the axial hydrogen on the other methylene carbon is axial below the ring system. The right half of the ring system is not identical to the left half, giving rise to two asymmetrical enantiomers. As molecules which are direct

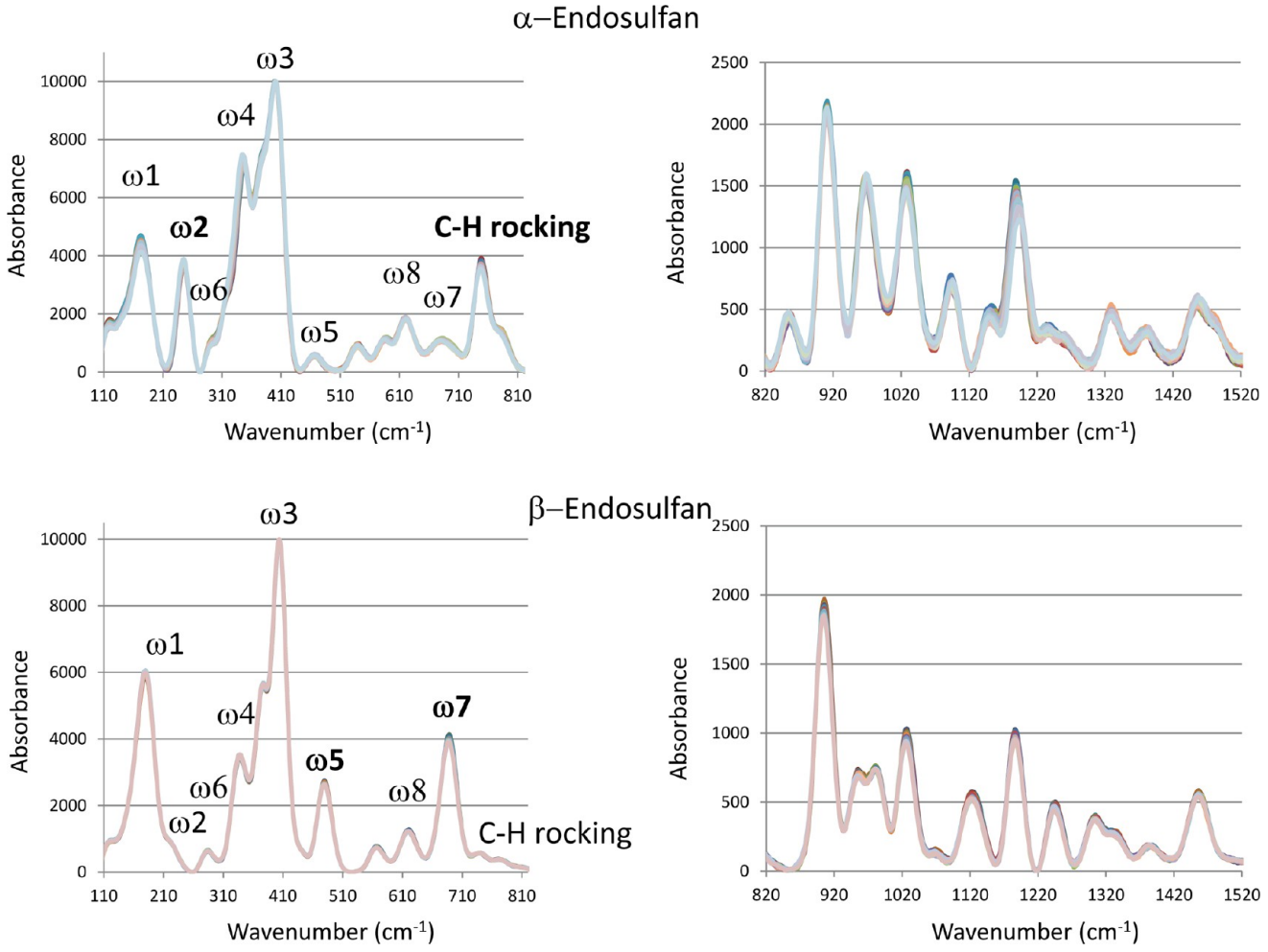

Figure 2. Raman spectra from 110 to 820 cm^{-1} and 820 to 1520 cm^{-1} acquired at 1 °C intervals from 50 to 102 °C for nearly pure α-endosulfan and for essentially pure β-endosulfan. Vibrational modes, ω1 through ω8 (Table 1), and C−H rocking, in the 110−820 cm^{-1} range are indentified. Relative intensities of each vibrational mode in the individual isomers were essentially temperature independent.

mirror images of each other, the two α-endosulfans will have identical Raman spectra.

Raman spectra were acquired at 1 °C intervals from 50 to 102 °C for nearly pure α-endosulfan and for essentially pure β-endosulfan; four major differences in the 110−810 cm^{-1} region were observed (Figure 2). Two major peaks were found in the α-endosulfan spectra at 229 cm^{-1} (ω2) and 748 cm^{-1} but were very weak in the spectra of β-endosulfan, whereas peaks seen in the β-endosulfan spectra at 460 cm^{-1} (ω5) and 686 cm^{-1} (ω7) were weak in the α-endosulfan spectra. Differences were also observed in the Raman fingerprint region, 820−1520 cm^{-1}. None of the peaks in the spectra of each nearly pure isomer showed a major change in intensity as a function of temperature.

From the work of Bocian and Strauss,[23] eight modes in the ring frequency region, 110−700 cm^{-1}, were assigned corresponding to the four symmetrical vibrational modes (ω1, ω3, ω5, and ω7) and to four asymmetrical vibrational modes (ω2, ω4, ω6, and ω8) (Table 1). Ring frequencies involve only the atoms in the ring, not the hydrogens bound to the carbons in the ring or the oxygen not part of the ring. Four of these vibrational modes represent changes in dipolar moment within the ring, that is, ω1, ω2, ω3, and ω4 correspond to changes in electron density among the ring atoms. Modes ω1 and ω3 represent symmetrical dipolar changes with respect to O−S−O, whereas modes ω2 and ω4 are asymmetrical. The asymmetrical dipolar moment ω2 is extremely weak in β-endosulfan. The other four vibrational modes correspond to ring-bending, ω5, ω6, ω7, and ω8. Modes ω5 and ω7 are symmetrical movements of the ring, and because α-endosulfan is asymmetrical, these modes are extremely weak. Asymmetrical ring-bending is depicted modes ω6 and ω8 and are weak peaks in the symmetrical β-endosulfan.

The modes observed in the fingerprint region of 720−1520 cm^{-1} correspond to the molecular vibrations of C−H. These movements include asymmetrical and symmetrical stretching, rocking, twisting, scissoring, and wagging. A peak at 748 cm^{-1} was observed in only α-endosulfan and corresponds to an asymmetrical C−H rocking movement. The remaining modes observed in the spectra of the pure isomers were difficult to assign unambiguously to specific atom vibrations.

Raman Spectra Mode Assignments for a 60:40 Mixture of α-Endosulfan:β-Endosulfan. Under similar gradient conditions for the individual isomers, Raman spectra were acquired at 1 °C intervals from 50 to 102 °C for a 60:40 mixture of α-endosulfan:β-endosulfan. The same eight ring vibrational modes, ω1−ω8, were observed in the 110−710 cm^{-1} range (Table 1; Figure 3). The peak which was only seen in the α-endosulfan spectra, 748 cm^{-1}, was also present in the

dx.doi.org/10.1021/jf404404w | J. Agric. Food Chem. 2014, 62, 2023−2030

Table 1. Assigned Vibrational Modes Observed in α-Endosulfan, β-Endosulfan, and a 60:40 Mixture α:β[a]

Vibrational Modes	Symmetry [1]	α-Endosulfan [2] (cm^{-1})	β-Endosulfan [2] (cm^{-1})	Mixture [2,3] (cm^{-1})
Dipolar Moment				
 ω1	S	169 s	177 s	174 - 180 s
 ω3	S	396 vs	401 vs	401 s
 ω2	A	240 s	223 vw	234 - 249 s
 ω4	A	339 vs	337 s	342 - 345 s
Ring Movement				
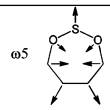 ω5	S	460 w	476 s	476 s
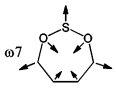 ω7	S	678 vw	686 s	683-689 s
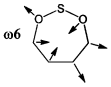 ω6	A	289 w	281 w	289 w
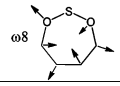 ω8	A	616 w	619 w	619 s

[a]Assignments were made using the vibrational modes observed in the structural analogue, 1,3-dioxepane.[23]. [1]A = asymmetrical, S = symmetrical. [2]vs = very strong, s = strong, w = weak, vw = very weak. [3]60:40 mixture of α-endosulfan:β-endosulfan.

mixture, as well as the peak corresponding to C−Cl vibration at 378 cm^{-1}. The intensity of these modes remained essentially unchanged as a function of temperature until 88 °C, after which some temperature dependence in some peaks was observed. Peaks corresponding to ω2 and ω8 increased by approximately 10%, while the peak intensity of ω1 decreased by 26%. Two additional small peaks which displayed some temperature dependence were observed at 542 and 590 cm^{-1} but were not assigned.

In the more flexible fingerprint of 720−1520 cm^{-1}, temperature dependency was much more dramatic (Figure 3). Below 97 °C, temperature had little effect on peak intensity, however, above 97 °C, intensity of several modes increased substantially, indicating that these sites in the molecules of one or both isomers were more flexible and therefore absorbed the increased thermal energy. Using the assignments of Bocian and Strauss,[23] Anconi et al.,[24] and Artur et al.,[25] the vibrational modes were identified, however, these peaks cannot be assigned definitively to one or both isomers. The intensity of the peaks at 907 cm^{-1} (C−H rocking) increased by 12%, at 968 cm^{-1} (ring expansion and C−H rocking) increased by 70%, and at 1028 cm^{-1} (ring expansion and bending) increased by 35%. Larger peak intensity increases of 140% and 200% were observed at 1092 cm^{-1} (ring expansion and mixed C−H motions) and 1350 cm^{-1} (C−H wagging and twisting), respectively.

These observations indicate that the nonuniform molecular surroundings of the mixture allow for temperature dependent changes in the intensity of vibrational movements which are not observed in the pure isomers. Furthermore, the nonuniform molecular surroundings allow for the intensity of asymmetrical ring frequencies to increase and, correspondingly, the symmetrical ring frequencies to decrease in intensity. At temperatures at 150 °C and above, pure β-endosulfan begins to exhibit isomerization as a result of formation of a nonuniform molecular environment caused by the changes in the lattice structure (phase change) of the pure compound.[18]

Contour Plots of TDR Spectra. Contour plots of temperature as a function of frequency (wavenumber) and spectral density were developed for the Raman spectral data of the 60:40 mixture and are shown over the temperature range of 88−102 °C and for the wavenumbers of 110−1500 cm^{-1} (Figure 4). These plots provide a more facile visualization of the data and enable identification of concurrent changes in frequency and intensity within the temperature gradient. If the frequency of a specific peak changes with increasing temperature, the slope of the line band will change, and if no changes occur in the frequency, the band will appear vertical in the plot. Spectral density (peak intensity) is represented by color change moving from cool colors (blue to green) to warmer colors (yellow to orange to red) as intensity increases. Over this temperature range, several vibrational modes were essentially temperature independent, ω3, ω4, ω7, and C−H rocking at 748 cm^{-1}.

For all the remaining modes, discrete temperature dependent changes occurred above 97 °C. Slight intensity increases, peak broadening, and peak shifting were observed for ω2, ω8, and C−H rocking at 907 cm^{-1}, while the peak at ω1 narrowed and decreased in intensity somewhat. The most dramatic changes occurred at 970, 1027, 1092, and 1350 cm^{-1}, where spectral density increased, peaks shifted, and peaks broaden substantially as the temperature increased. The response of these four vibrational modes indicate that these molecular sites are the most sensitive to the temperature (i.e., absorption of thermal energy) and are, therefore, the most flexible.

Correlating TDR Observations with Phase Transition Data. DSC is used to measure thermal absorption based upon aggregates of molecules, or macroscopic properties, such as melting, boiling, and sublimation, changes in crystal lattice structure, or isomerization. In contrast, Raman spectroscopic data provide information about molecular changes that take place at specific molecular sites and may or may not be involved in molecular aggregation/macroscopic changes. While TDR and DSC do not necessarily measure the same physical phenomenon, when the temperature dependence over a specific temperature gradient between the two does correlate, the macroscopic and molecular properties presumably overlap.

DSC data were collected over a temperature range of 50.0−110 °C and have been presented elsewhere.[20] A phase transition for α-endosulfan was observed at 90−96 °C with a maximum at 93 °C, whereas, for β-endosulfan, a phase transition was seen at 97−102 °C. A much broader range in the phase transition temperature occurred in a 60:40 mixture of α-endosulfan:β-endosulfan beginning at 80 °C and ending at 104 °C, with a maximum at 94 °C. The DSC results identify the discretely different temperature ranges over which thermal absorption of the individual endosulfan isomers occurs. The phase transition seen at 97−102 °C for β-endosulfan corresponds to the largest spectral differences in the TDR spectra. Therefore, the observed temperature-dependent

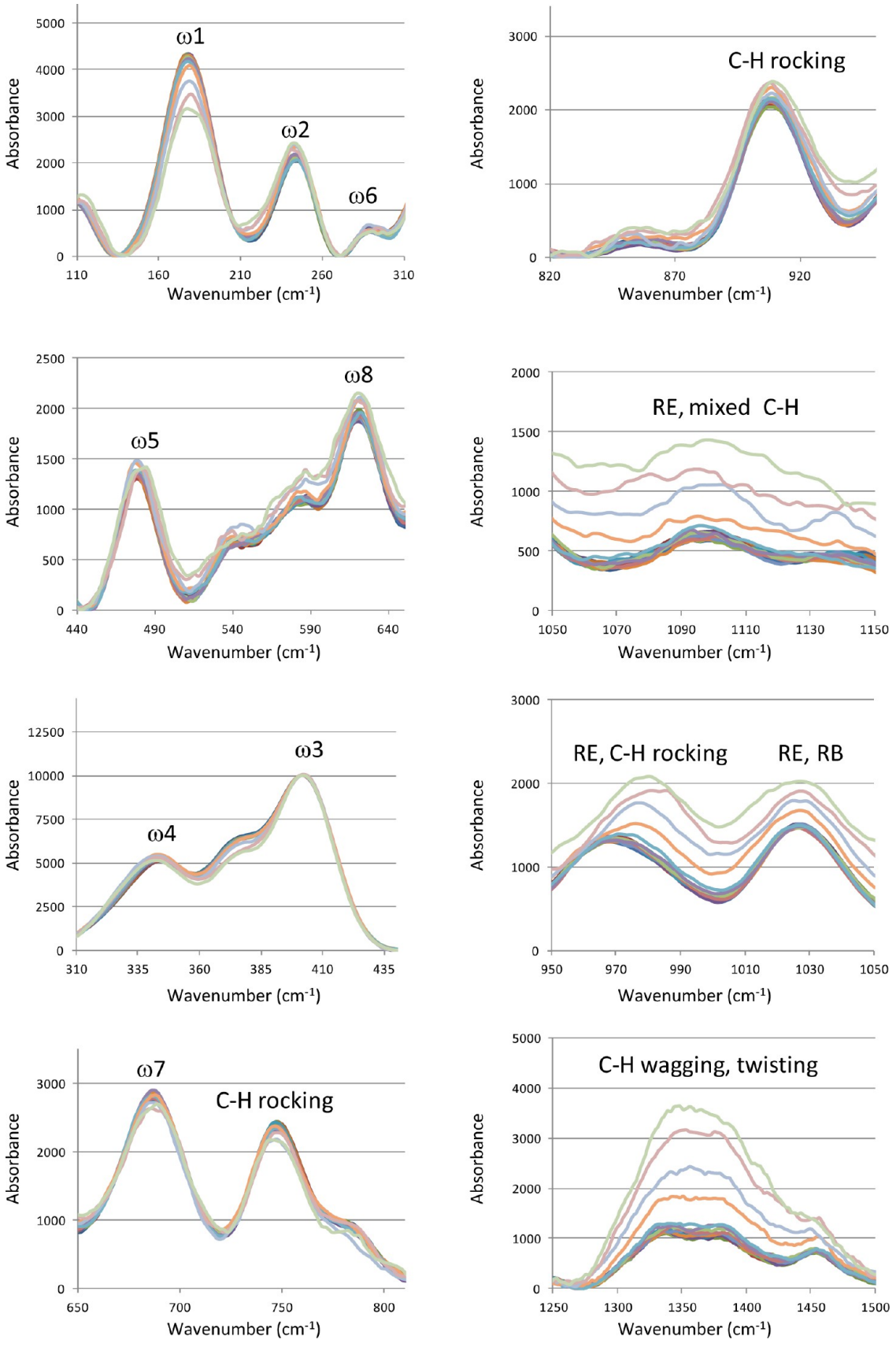

Figure 3. Raman spectra from 110 to 1520 cm^{-1} acquired at 1 °C intervals from 50 to 102 °C for a mixture of 60:40 α-endosulfan:β-endosulfan; each line represents a spectrum at an individual temperature. Vibrational modes are identified: ω1 through ω8 (Table 1), C−H rocking, wagging, and twisting, ring expansion (RE), and ring bending (RB). Relative intensities of each vibrational mode were essentially temperature independent until 97 °C. Noticeable temperature dependence was observed for vibrational modes at 177, 970, 1027, 1092, and 1350 cm^{-1}.

dx.doi.org/10.1021/jf404404w | J. Agric. Food Chem. 2014, 62, 2023−2030

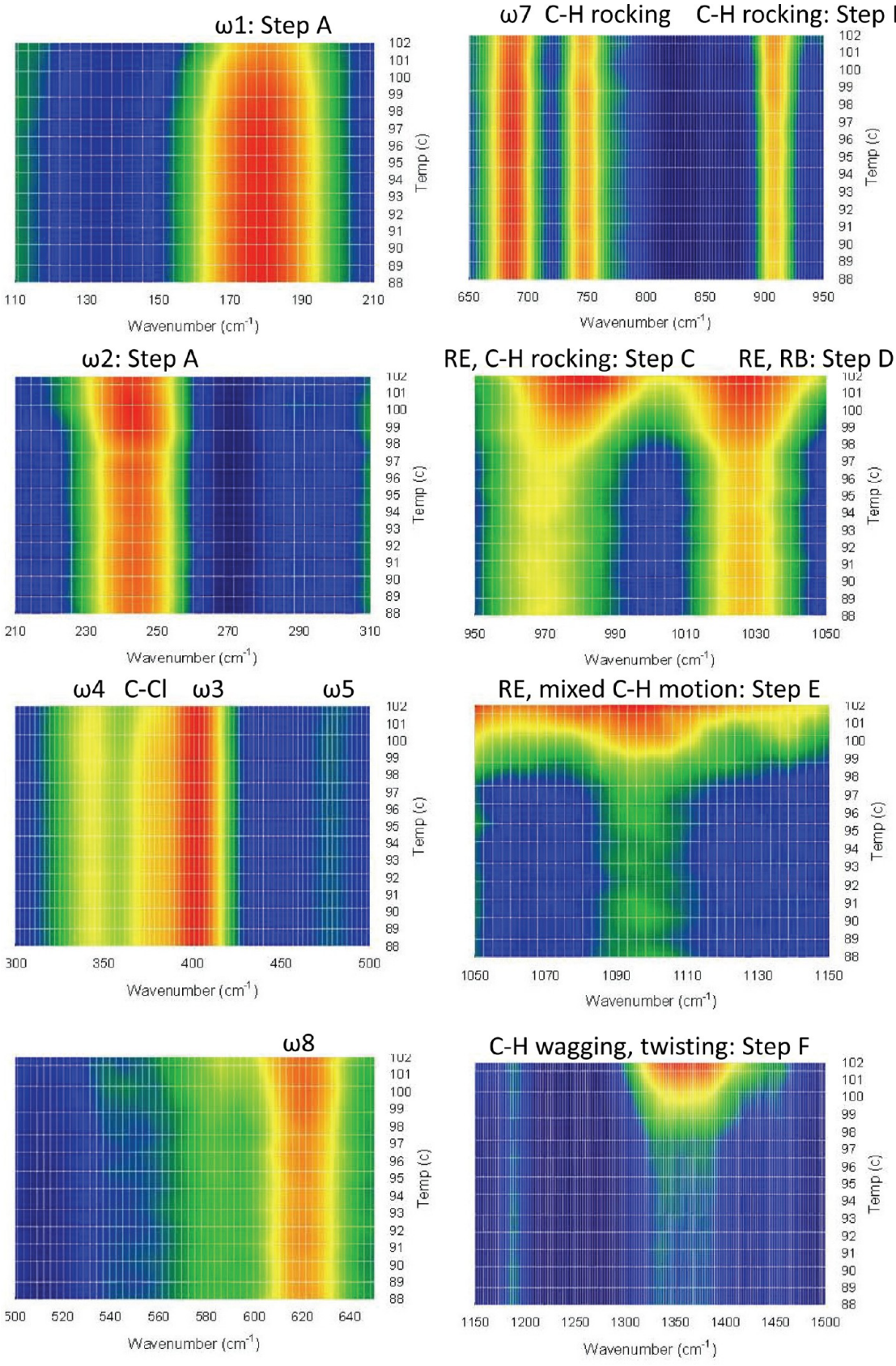

Figure 4. Contour plot of temperature as a function of frequency (wavenumber) and spectral density for the Raman spectral data of a 60:40 mixture of α-endosulfan:β-endosulfan over the temperature range of 88−102 °C and for the wavenumbers of 110−1500 cm^{-1}. Spectral density (peak intensity) is represented by color change moving from cool colors (blue to green) to warmer colors (yellow to orange to red) as intensity increases. Vibrational modes are identified as well as the mechanistic steps A−F of β-endosulfan isomerization to α-endosulfan.

dx.doi.org/10.1021/jf404404w | J. Agric. Food Chem. 2014, 62, 2023−2030

Raman spectral changes are due to changes in β-endosulfan not α-endosulfan.

Mechanism for Isomerization of β-Endosulfan to α-Endosulfan. Using the identified vibrational modes and the temperature dependence data, the mechanism for β-endosulfan isomerization to α-endosulfan becomes readily apparent (Figure 5). At 97 °C, the asymmetrical electron density

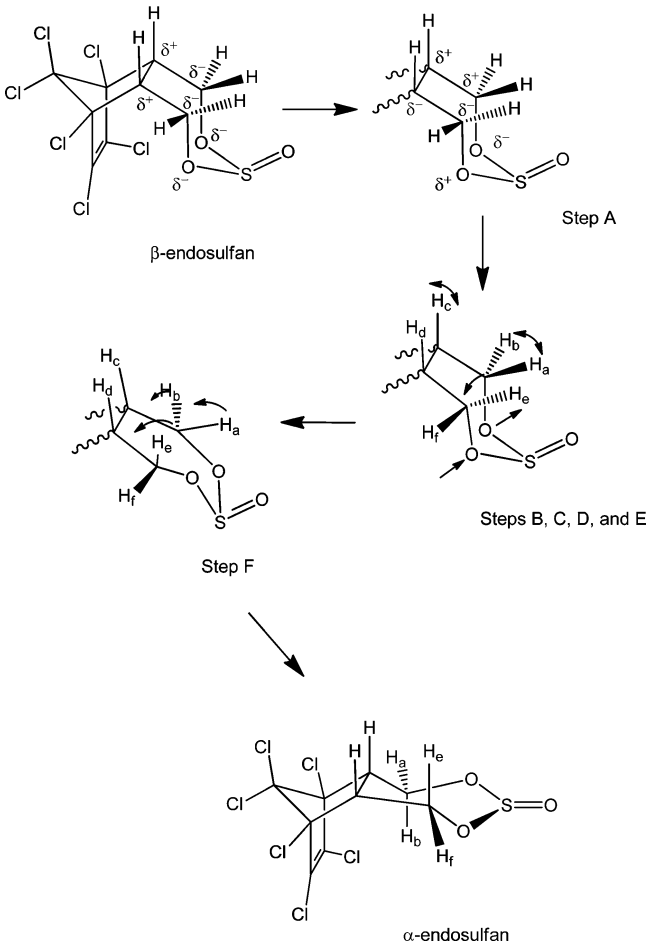

Figure 5. Mechanism steps A–F of β-endosulfan isomerization to α-endosulfan.

distribution in the seven-membered ring, ω2, begins to increase, and a corresponding decrease in the symmetrical electron density distribution, ω1, is observed (step A). Concurrently, the C–H rocking of the methylene carbons at 908 cm^{-1} increases (step B), followed by additional increases vibrational modes in C–H rocking and ring expansion at 970 cm^{-1} (step C) and ring expansion and ring bending at 1028 cm^{-1} (step D). At 99 °C, ring expansion and mixed C–H motions vibrational modes at 1092 cm^{-1} broaden substantially (step E). The final C–H wagging and twisting at 1350 cm^{-1} causes the methylene carbon to "flip", affording α-endosulfan (step F). From these data, we conclude that the reverse process of α-endosulfan isomerization to β-endosulfan is precluded.

This mechanism provides a rationale for the lack of changes in the TDR of nearly pure β-endosulfan. In the symmetrical crystal lattice of solid β-endosulfan, the symmetrical vibrational modes ω1 and ω3 are most dominant, while the asymmetrical vibrational mode ω2 is very weak (Table 1). An asymmetrical molecular surrounding appears to be critical to isomerization of β-endosulfan, as is the case in the mixture of α-endosulfan and β-endosulfan.

Relevance to the Environmental Fate of Endosulfan. In the environment, α- and β-endosulfan do not exist as pure compounds and β-endosulfan is not bound by the crystal lattice structure which inhibits isomerization. Therefore, with sufficient energy applied, isomerization of β- to α-endosulfan can occur in environmental matrices. Results presented here including the combination of DSC and TDR indicate that isomerization from α- to β-endosulfan does not occur and this process should not be observed in the environment. However, two publications have provided evidence of isomerization from α- to β-endosulfan under environmentally relevant conditions.[26,27]

The first publication describes application of individual isomers to field plots of a chickpead crop (three plots per isomer).[26] Leaf samples were collected just after application and periodically over a 15 day period. The specific purity of the solution was not reported, only that "pure" β-endosulfan was used. In the α-endosulfan-applied plots, after 7 days, 83% dissipation of α-endosulfan was observed and 2% β-endosulfan and 17% endosulfan sulfate was detected. In the β-endosulfan-applied plots, after 7 days 52% dissipation of β-endosulfan was observed and 8% α-endosulfan and 42% endosulfan sulfate was detected. The small contribution from β-endosulfan in the α-endosulfan applied plots was likely due to impurities in the original solution. Commercially available standards of endosulfan isomers are rarely 100% pure and typically contain traces of the other isomer. Because the specific purities of the starting solutions were not reported and a complete mass balance was not obtained, conclusions regarding isomerization cannot be confirmed.

The second publication[27] examined the fate of endosulfan and the formation of degradation products in estuarine mesocosms. Mesocosms were spiked separately with α-endosulfan, β-endosulfan, or the technical mixture of 70:30 α- to β-endosulfan. The purity of the single isomer standards is listed as 99.99% as determined by gas chromatography electron capture detection. Water samples were collected over a 100 h period and analyzed for both isomers and degradation products. For the β-endosulfan applied mesocosm, loss was listed as 96.9 ± 0.3%, with approximately 84% mass recovered. The authors list 2.1 ± 0.1% α-endosulfan detected. In the α-endosulfan applied mesocosm, the loss of α-endosulfan was listed as 93.6 ± 0.4%, with approximately 60% mass recovered. The percentage of β-endosulfan detected was 0.7 ± 0.1%. The percentage of β-endosulfan detected in the α-endosulfan-applied mesocosm was less than 1% and could be attributed to contamination in the original spiking material when taking into account the typical level of variability in gas chromatography–mass spectrometry analysis.

The only other published paper that has reported isomerization of α- to β-endosulfan is Guerrini et al.[28] The authors utilized surface-enhanced Raman scattering (SERS) to analyze the two isomers in their pure form as solids and then α-endosulfan as complexed with charged Ag nanoparticles coated with an organic compound (bis-acridinium lucigenin). Isomerization of α- to β-endosulfan was reported based on comparison of SERS spectral data. The SERS spectral data for the complexed α-endosulfan is reported to indicate weakening of bands associated with α-endosulfan and intensification of bands associated with β-endosulfan. However, background interferences from the bis-acridinium lucigenin coating were subtracted

from the spectra of the nanoparticle complexes, leading to a negative peak in a critical region of the spectra. No other confirmatory data concerning presence of β-endosulfan were discussed. Therefore, α- to β-endosulfan isomerization cannot be conclusively identified.

AUTHOR INFORMATION

Corresponding Author

*E-mail: cathleen.hapeman@ars.usda.gov.

Funding

This work was supported financially by U.S. Department of Agriculture, Agricultural Research Service intramural projects: 1265-42000-018-00 and 1265-12610-001-00.

Notes

Mention of specific products is for identification and does not imply endorsement by the U.S. Department of Agriculture to the exclusion of other suitable products or suppliers.
The authors declare no competing financial interest.

ABBREVIATIONS USED

DSC, differential scanning calorimetry; POP, persistent organic pollutants; RE, ring expansion; RB, ring bending; TDR, temperature-dependent Raman; UNEP, United Nations Environmental Programme

REFERENCES

(1) Maier-Bode, H. Properties, effect, residues and analytics of the insecticide endosulfan. *Residue Rev.* **1968**, *22*, 1−44.

(2) *EPA Action to Terminate Endosulfan*; United States Environmental Protection Agency: Washington, DC, June 2010; http://www.epa.gov/pesticides/reregistration/endosulfan/endosulfan-cancl-fs.html#decision (Accessed September 20, 2013).

(3) Lubick, N. Endosulfan's exit: U.S. EPA pesticide review leads to a ban. *Science* **2010**, *328*, 1466.

(4) *Endosulfan Phase-Out*; United States Environmental Protection Agency: Washington, DC, November, 2010; http://www.epa.gov/pesticides/reregistration/endosulfan/endosulfan-agreement.html (Accessed September 20, 2013).

(5) *United Nations Targets Widely-Used Pesticide Endosulfan for Phase Out*; United Nations Environment Programme: Geneva, May 3, 2011; http://chm.pops.int/TheConvention/Media/PressReleases/COP5Geneva,3May2011Endosulfanphaseout/tabid/2216/Default.aspx (Accessed September 20, 2013).

(6) Weber, J.; Halsall, C. J.; Muir, D.; Teixeira, C.; Small, J.; Solomon, K.; Hermanson, M.; Hung, H.; Bidleman, T. Endosulfan, a global pesticide: a review of its fate in the environment and occurrence in the Arctic. *Sci. Total Environ.* **2010**, *408*, 2966−2984.

(7) Becker, L.; Scheringer, M.; Schenker, U.; Hungerbühler, K. Assessment of the environmental persistence and long-range transport of endosulfan. *Environ. Pollut.* **2011**, *159*, 1737−1743.

(8) Janssen, M. P. M. *Endosulfan. A Closer Look at the Arguments against a Worldwide Phase Out*; RIVM Letter Report 601356002/2011; National Institute for Public Health and the Environment: Bilthoven, Netherlands, 2011; 92 pp, http://www.rivm.nl/bibliotheek/rapporten/601356002.pdf (Accessed September 20, 2013).

(9) Riemschneider, R.; Hilscher, J. C. Thiodan und analoge Verbindungen IV: Zur Kenntnis der Thiodan-Isomerie. *Z. Naturforsch., B: Chem. Sci.* **1960**, *15*, 809−810.

(10) Riemschneider, R.; Wuscherpfennig, V. Über den räumlichen Bau der Thiodan-Isomeren. *Naturwissenschaften* **1961**, *48* (5), 130−131.

(11) Riemschneider, R.; Wucherpfennig, V. Thiodan und analoge Verbindungen, 7. Konstellationen und Dipolmomente isomerer Thiodane. *Z. Naturforsch., B: Chem. Sci.* **1962**, *17*, 723.

(12) Forman, S. E.; Durbetaki, A. J.; Cohen, M. V.; Olofson, R. A. Conformational equilibria in cyclic sulfites and sulfates. The configurations and conformations of the two isomeric thiodans. *J. Org. Chem.* **1965**, *30*, 169−175.

(13) Schmidt, W. F.; Hapeman, C. J.; Fettinger, J. C.; Rice, C. P.; Bilboulian, S. Structure and asymmetry in the isomeric conversion of β- to α-endosulfan. *J. Agric. Food Chem.* **1997**, *45*, 1023−1026.

(14) Rice, C. P.; Chernyak, S. M.; Hapeman, C. J.; Bilboulian, S. Air−water distribution of the endosulfan isomers. *J. Environ. Qual.* **1997**, *26*, 1101−1106.

(15) Rice, C. P.; Chernyak, S. M.; McConnell, L. L. Henry's law constants for pesticides measured as a function of temperature and salinity. *J. Agric. Food Chem.* **1997**, *45*, 2291−2298.

(16) Simonich, S. L.; Hites, R. A. Global distribution of persistent organochlorine compounds. *Science* **1995**, *269*, 1851−1854.

(17) Burgoyne, T. W.; Hites, R. A. Effects of temperature and wind direction on the atmospheric concentrations of α-endosulfan. *Environ. Sci. Technol.* **1993**, *27*, 910−914.

(18) Schmidt, W. F.; Bilboulian, S.; Rice, C. P.; McConnell, L. L.; Fettinger, J. C.; Hapeman, C. J. Thermodynamic, spectroscopic, and computational evidence for the irreversible conversion of β- to α-endosulfan. *J. Agric. Food Chem.* **2001**, *49*, 5372−5376.

(19) Walse, S. S.; Shimizu, K. D.; Ferry, J. L. Surface-catalyzed transformations of aqueous endosulfan. *Environ. Sci. Technol.* **2002**, *36*, 4846−4853.

(20) Schmidt, W. F., Nguyen, J. K., Qin, J., Kim, M. S., Mookherji, S., McConnell, L. L., Hapeman, C. J. DSC and Raman spectra of α- and β-endosulfan plus 60/40 mixture. In *SPIE Defense, Security, and Sensing*; International Society for Optics and Photonics: Bellingham, WA, May 2013; pp 87210R-1−87210R-7.

(21) Qin, J.; Chao, K.; Kim, M. S. Raman chemical imaging system for food safety and quality inspection. *Trans. ASABE* **2010**, *53*, 1873−1882.

(22) Moore, W. H.; Ching, J. H. C.; Warrier, A. V. R.; Krimm, S. Assignment of torsion and low frequency bending vibrations of secondary chlorides. *Spectrochim. Acta, Part A* **1973**, *29*, 1847−1858.

(23) Bocian, D. F.; Strauss, H. L. Vibrational spectra, conformations, and potential functions of cycloheptane and related oxepanes. *J. Am. Chem. Soc.* **1977**, *99*, 2866−2878.

(24) Anconi, C. P. A.; Nascimento, C. S., Jr.; Dos Santos, H. F.; DeAlmeida, W. B. A highly correlated ab initio investigation of the temperature dependent conformational analysis of cycloheptane. *Chem. Phys. Lett.* **2006**, *418*, 459−466.

(25) Artur, C.; Le Ru, R. C.; Etchegoin, P. G. Temperature dependence of the homogeneous broadening of resonant Raman peaks measured by single-molecule surface-enhanced Raman spectroscopy. *J. Phys. Chem. Lett.* **2011**, *2*, 3002−3005.

(26) Gopal, M.; Mukherjee, I. Determination of residues of endosulfan and endosulfan sulfate on eggplant, mustard and chickpea. *Pestic. Sci.* **1994**, *37*, 67−72.

(27) Walse, S. S.; Scott, G. I.; Ferry, J. L. Stereoselective degradation of aqueous endosulfan in modular estuarine mesocosms: formation of endosulfan γ-hydroxycarboxylate. *J. Environ. Monit.* **2003**, *5*, 373−379.

(28) Guerrini, L.; Aliaga, A. E.; Carcamo, J.; Gomez-Jeria, J. S.; Sanchez-Cortes, S.; Campo-Vallette, M. M.; Garcia-Ramos, J. V. Functionalization of Ag nano-particles with the bis-acridinium lucigenin as a chemical assembler in the detection of persistent organic pollutants by surface-enhanced Raman scattering. *Anal. Chim. Acta* **2008**, *624*, 286−293.